Journal of Physics D: Applied Physics

PAPER • **OPEN ACCESS**

Optimisation of plasma processes for decontamination of bacterial contaminants on polymeric food packaging materials

To cite this article: Caterina Maccaferri *et al* 2025 *J. Phys. D: Appl. Phys.* **58** 055202

OPEN ACCESS
IOP Publishing
Journal of Physics D: Applied Physics
J. Phys. D: Appl. Phys. **58** (2025) 055202 (12pp)
https://doi.org/10.1088/1361-6463/ad8d63

Optimisation of plasma processes for decontamination of bacterial contaminants on polymeric food packaging materials

Caterina Maccaferri[1,4], **Francesco Tomelleri**[1,4], **Matteo Gherardi**[1,2] and **Romolo Laurita**[1,3,*]

[1] Department of Industrial Engineering, Alma Mater Studiorum. Università di Bologna, Bologna, Italy
[2] Advanced Mechanics and Materials, Interdepartmental Center for Industrial Research (AMM-ICIR), Alma Mater Studiorum—Università di Bologna, Bologna, Italy
[3] Interdepartmental Centre for Industrial Research Health Sciences and Technologies, Alma Mater Studiorum—Università di Bologna, Ozzano dell'Emilia, Italy

E-mail: romolo.laurita@unibo.it, caterina.maccaferri3@unibo.it, francesco.tomelleri@unibo.it and matteo.gherardi4@unibo.it

Received 20 June 2024, revised 11 September 2024
Accepted for publication 31 October 2024
Published 19 November 2024

Abstract

Foodborne diseases present a global health challenge, with over 420 000 deaths annually. Packaging plays a vital role in food safety but can introduce hazards if contaminated. Traditional decontamination methods are energy-intensive or leave toxic residues. Cold plasma technology offers promising solutions for generating antimicrobial reactive species. This study optimises a plasma system for packaging decontamination, achieving high inactivation rates for *Staphylococcus epidermidis* (gram-positive) and *Acinetobacter baumannii* (gram-negative), respectively 3.5 and 4.7. Statistical analysis guide process optimisation, highlighting factors enhancing biocidal action: treatment chamber size reduction, high duty cycle, and mist injection. The system proves effective against both kinds of bacteria, with gram-negative bacteria showing higher sensitivity. The study focuses on optimising an innovative process, emphasising the process towards industrialisation and highlighting economic and environmental benefits. This investigation's innovative approach aims to bridge the gap between laboratory prototypes and industrial applications.

Supplementary material for this article is available online

Keywords: surface dielectric barrier discharge, food industry, nuclear technology, plasma technology, atmospheric pressure cold plasma, decontamination

[4] These authors contributed equally to this work.
[*] Author to whom any correspondence should be addressed.

1. Introduction

Foodborne diseases, i.e. the over 200 different illnesses caused by contaminated food, pose a significant global health challenge, causing more than 420 000 deaths annually (WHO 2014). Despite foodborne illnesses still being a poverty-related issue, mainly affecting developing countries, all geographic areas are afflicted due to globalisation and climate change. The European Union (EU) reports thousands of foodborne outbreaks annually, recalling the interest in food safety (European Food Safety Authority 2023). From this perspective, food packaging plays a vital role in preserving food quality and safety by acting as a protective barrier against external contaminants (Hoover 2001). However, packaging materials themselves can introduce hazards if not properly managed; contaminated packaging can lead to food contamination, so appropriate decontamination techniques should be employed (Piergiovanni and Limbo 2017). Traditionally, thermal methods are widely used, including use of dry heat or hot steam. Of course, these methods are energy-consuming and not suitable for heat-sensitive materials. Another option is chemical agents such as hydrogen peroxide, but their supply and disposal costs are high from an economic and environmental point of view; furthermore, they can leave toxic residues on the materials. Finally, physical methods are attracting increasing interest. Among these, cold plasma technology offers promising solutions for food-contact surfaces decontamination (Mandal *et al* 2018, Feizollahi *et al* 2021, Maccaferri *et al* 2024a). Cold atmospheric plasmas (CAP) generate active chemical components, including reactive oxygen and nitrogen species (RONS), which possess antimicrobial properties. RONS can interact with biomolecules through different mechanisms, resulting in protein modification by hydroxylation, dehydrogenation, nitration, and dimerisation of sensible aminoacids (Takai *et al* 2014); lipid cleavage, oxidation, and membrane permeability enhancement (Leduc *et al* 2009, Yusupov *et al* 2017); nucleic acid lesions through nucleotide oxidation, strands break and cross-linking (Cadet *et al* 2011, 2012, Szili *et al* 2017). Other biocidal agents, such as heat, radiation, and electromagnetic fields, are involved in plasma generation. All these components deactivate microorganisms on food and packaging surfaces, making CAPs a suitable and innovative technology for food safety. A variety of different CAP systems configurations have been tested on polymeric packaging contaminated by bacteria (Maccaferri *et al* 2024a), including corona devices (Sipoldova and MacHala 2011, Kovalová *et al* 2013, Kordová *et al* 2018), dielectric barrier discharge (DBD) sources (Muranyi *et al* 2010, Yun *et al* 2010, Hu and Guo 2012, Kim *et al* 2014, Edelblute *et al* 2016, İbiş *et al* 2016, Kramer *et al* 2016, 2020, Zimmerman *et al* 2016, Govaert *et al* 2018), plasma jets (Deng *et al* 2010, Lee *et al* 2011, Noriega *et al* 2011, Cahill *et al* 2014, Kramer *et al* 2022), and surface DBD configurations (Hähnel *et al* 2010, Kleinschmidt *et al* 2015, Tučeková *et al* 2016, 2021, Bauer *et al* 2017, Salgado *et al* 2021, Maccaferri *et al* 2023), providing versatile options for food industry applications.

In this study, an optimisation process of a plasma system for surface decontamination is presented. The efficacy assessment at each process step aims to identify the best combination of factors to enhance the biocidal action. The selected factors were treatment chamber size, input power and a possible mist injection.

2. Materials and methods

2.1. Plasma system

A large-area surface dielectric barrier discharge source (AlmaPlasma s.r.l., Bologna, Italy) was used to treat the contaminated samples indirectly. The main components, previously illustrated by (Maccaferri *et al* 2023), are 4 high-voltage electrodes embedded in resin, a grounded perforated metal sheet, and a thin dielectric layer sandwiched between the opposite-pole electrodes.

A sinusoidal high-voltage generator (AlmaPlasma s.r.l., Bologna, Italy) operating at a frequency of 23 kHz and a peak-to-peak voltage of 14 kV supplied the plasma source (figure 1). The average dissipated power in the discharge was 190 ± 1.6 W with DC 100% (duty cycle (DC), i.e. the ratio between the on time of the generator over the sum of on and off time), resulting in a surface power density equal to 1.25 W cm^{-2}, as reported in the previous study.

The plasma source worked as the lid of the treatment chamber, confining the interior atmosphere during treatments. Two different PVC treatment chambers were used: a larger one, with internal dimensions of $25 \times 37 \times 20$ cm (volume 18.5 l), and a thinner one, with internal dimensions of $25 \times 37 \times 1$ cm (0.925 l), hereinafter referred to respectively as 'wide' and 'narrow' chambers.

The system was designed to work in ambient conditions.

A water aerosol injection system was implemented to evaluate the effect induced by the presence of water droplets, as depicted in figure 2. Liquid water was placed in a commercial aerosol nebuliser ampoule (Gima, Italy). The water droplets were conveyed by a compressed air flux passing through the ampoule and controlled by a fluxmeter (Riels Instruments, Italy) set at 3 NL min^{-1}. The volume of water injected in 10 min was equal to 1 ± 0.07 ml.

Whether or not mist was injected resulted in the test being referred to as 'Mist' (conducted as just described) or 'Dry' (under static ambient air conditions), respectively.

2.2. Evaluation of antimicrobial efficacy

The *Staphylococcus epidermidis* ATCC12228 and *Acinetobacter baumannii* ATCC 1927 inocula were cultured on tryptic soy agar (TSA) (VWR International, Belgium) for 24 h at 37 °C to produce master plates. An aliquot from these plates was then suspended and adjusted in PBS (Corning, USA) (*S. epidermidis*) or deionised water (DIW) (Monaco, Italy) (*A. baumannii*) to obtain a master suspension (MS) with a concentration of 10^7–10^8 CFU ml^{-1}, confirmed by an

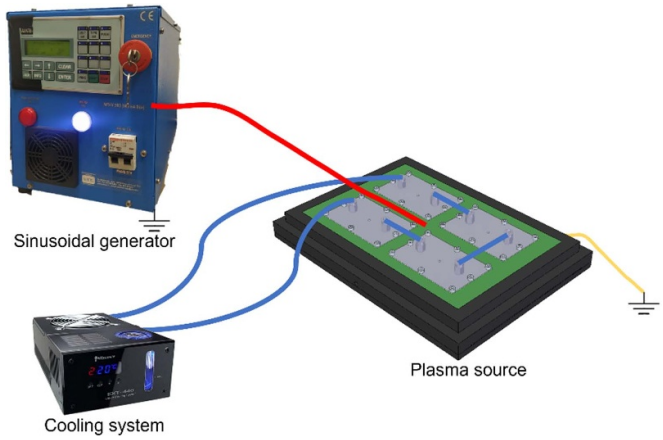

Figure 1. Scheme of the plasma system.

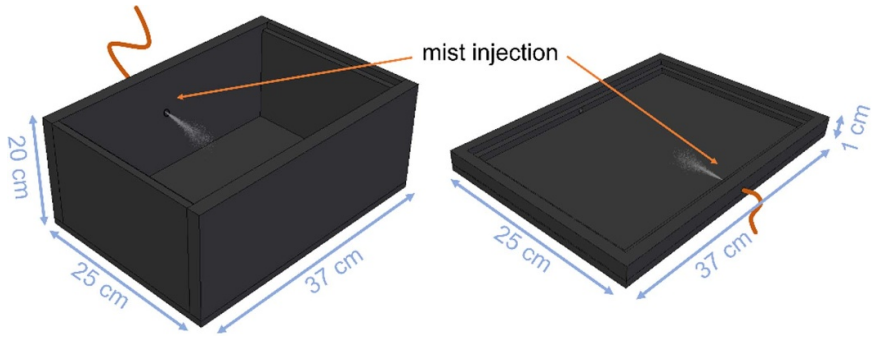

Figure 2. Geometries of the two treatment chambers and mist injection positions.

OD600 reading of 0.200 ± 0.003, measured using a spectrophotometer (FullTech Instruments, Italy).

Polypropylene disks (Ø 2.5 cm) sterilised with 70% ethanol (Sigma-Aldrich, USA) and UV light (Bio II Advance, Telstar, Japan), were contaminated with 20 drops of 1 μl of the MS and allowed to dry at 37 °C for 15 min. Both treated and controlled samples were contaminated in this manner.

Following plasma treatment, recovery steps were conducted. Each sample was vortexed for 2 min in PBS (*S. epidermidis*) or DIW (*A. baumannii*) containing 0.1% Tween 80 (Sigma-Aldrich, USA). *A. baumannii* recoveries were done by adding glass beads to the centrifuge tubes. The samples were then diluted and spread on agar plates. After 24 h of incubation at 37 °C, the number of colonies on the plates was counted.

The inactivation activity of plasma treatment was evaluated using the following formula:

$$\mathrm{Log}R = \mathrm{Log}N_0 - \mathrm{Log}N_t$$

where N_0 and N_t are the number of colony-forming units of control and plasma treated, respectively.

In order to perform mist and ROS scavenging treatments, respectively, water and a water solution of 5% w/v Sodium thiosulphate ($Na_2S_2O_3$) (VWR Chemical, Belgium), a widely used O_3 quencher (Yang *et al* 2020), was aerosolised in the treatment chamber. Control samples in these experiments were obtained by aerosolising $Na_2S_2O_3$ in the treatment chamber with no plasma generation.

2.3. Analytical determination

2.3.1. Optical absorption spectroscopy (OAS) and data processing. An optical absorption analysis has been carried out to comprehend the reactive species dynamics inside the treatment chamber. Two species were selected: nitrogen dioxide (NO_2) and ozone (O_3). Their kinetics was observed during treatments lasting 10 min under various operating conditions. The results are presented as the mean values (and standard errors) of instantaneous concentrations over the whole treatment time. The acquisition procedure and data processing were carried out as previously described by Maccaferri *et al* (2023) and Simoncelli *et al* (2019).

OAS utilises the Lambert–Beer law to quantify specific molecules by measuring absorption at particular wavelengths. This involves passing light through a region with target molecules, where absorption attenuates light intensity proportionally to molecule concentration. The set-up, illustrated in figure 3, includes lamps at specific wavelengths (255 nm for ozone, 400 nm for nitrogen dioxide), focused by lenses and directed into a spectrometer for analysis.

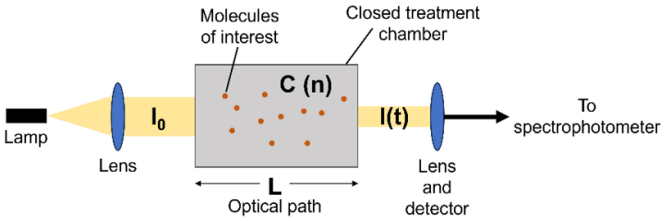

Figure 3. Schematic of set-up for OAS analysis.

The optical path chosen for the analysis was located in the centre of the largest side of the treatment chamber and it had a length of 25 cm. The passage of the light beam is provided by the presence of quartz windows (transparent at the investigated wavelengths) on the sides of the treatment chamber.

Residual light intensity ($I(t)$) was acquired during the whole plasma treatment, allowing the calculation of reactive species concentration, as a function of time, by means of Lambert–Beer law, as follows:

$$n_i = -\frac{1}{L \cdot \sigma_i} \cdot \ln\left(\frac{I(t)}{I_0}\right)$$

in which I_0 represents the initial light intensity, σ_i is the cross-section, i.e. a function of the wavelength specific of the chemical species, and L is the optical path. The wavelengths emitted by the lamp are chosen to maximise the cross-sections, in accordance with Moiseev *et al* (2014), obtaining the following values:

$$\sigma_{O3\_253\ nm} = 1.12{*}10^{-17}\mathrm{cm}^2$$

$$\sigma_{NO2\_400\ nm} = 6.4{*}10^{-19}\mathrm{cm}^2$$

which are respectively the maximum cross-section of ozone, obtained at 253 nm, and of nitrogen dioxide, obtained at 400 nm.

The OAS measurements are unfeasible with aerosol injection due to the interference of liquid droplets with the light beam. Consequently, the OAS results will be presented solely for 'Dry' operating conditions (meaning in the absence of mist injection).

2.3.2. Temperature measurements. In order to evaluate the plasma influence on the temperature of the samples (and immediately surrounding air) during treatments, thermal measurements in the different operating conditions were carried out. Three commercial fibre-optic sensors (MultiSens, OpSens, Canada) were placed inside the treatment chamber in contact with the same samples used for biological experiments and equally positioned. The probes were then connected to a detection device (MultiSens, OpSens, Canada) for data acquisition. The temperature was monitored for 10 min of plasma treatment under all the different operating conditions. Each measurement was repeated three times.

Table 1. Plasma treatment conditions.

Chamber size	Duty cycle	With mist injection	Without mist injection
Narrow	DC 100%	*S. epidermidis* *A. baumannii*	*S. epidermidis* *A. baumannii*
	DC 10%	*S. epidermidis*	*S. epidermidis*
Wide	DC 100%	*S. epidermidis*	*S. epidermidis*
	DC 10%	*S. epidermidis*	*S. epidermidis*

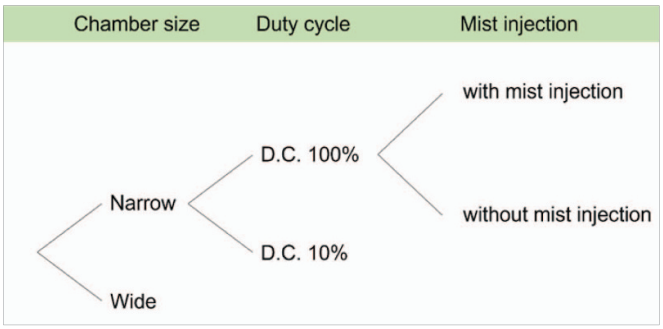

Figure 4. Optimisation path.

2.4. Plasma treatments

Three contaminated samples were placed inside the treatment chamber, lined up in the centre, for each replicate. The mist was possibly injected horizontally through a specific hole centred on the longest side of the chamber. Fourteen different treatments were carried out depending on the treatment chamber size, DC, possible mist injection and contaminant bacterial strain (table 1).

The DC was either 10% or 100%. These settings allow the system to work in the Ozone regime and Nitrogen oxides regime, respectively, according to our previous study (Maccaferri *et al* 2023).

The optimisation path is depicted in figure 4. At each successive step indicated in the top bar, there is a choice between the two factors listed just below. The path proceeds by selecting only the factors that optimise the effectiveness of the process while branching ceases towards less performing factors.

Each treatment consisted of a group of three simultaneously treated samples. Each treatment was repeated three times. Biological results which were not presented in the optimisation path but expressed in table 1 are reported as supplementary material.

2.5. Statistical analysis

All experiments were carried out in triplicates. Quantitative biological results are presented as mean value ± standard error of the mean. A Student's test was run to determine whether there were any statistically significant differences between the various outcomes (p-value < 0.05).

In order to evaluate the effects on the response of each factor involved and of their combination as well, a 2^3 design of experiment was adopted, as described by Montgomery (2013). This method enables the evaluation of each parameter independently, as well as the combined influence of multiple parameters on the outcome. This approach, typically employed in process optimisations, aims to gain insights into the interplay between the variables under investigation and their collective impact on the observed results. Each selected factor (treatment chamber size, DC, and the presence or absence of mist) includes low and high levels, as defined by the method. In this case, they were defined as follows:

(A) Chamber volume: narrow (low) and Wide (high),
(B) Presence or not of mist: dry condition (low) and mist injection (high),
(C) DC: 10% (low) and 100% (high).

The ANOVA (Analysis of variance) was performed to evaluate which factors and combinations cause a significant effect, with a threshold set at a p-value < 0.05. This statistical approach allowed us to discern the contributions of individual factors and their interactions, providing a comprehensive understanding of the experimental outcomes. By identifying significant effects and interactions, the authors aim to elucidate the key factors driving the observed responses and their combined impact on the studied phenomena.

3. Results and discussion

3.1. System optimisation for the inactivation of *Staphylococcus epidermidis*

Thanks to their cell wall configuration, Gram-positive bacteria display a higher resistance to classical treatments than Gram-negative bacteria (Breijyeh *et al* 2023). Therefore, a Gram-positive bacterial strain (*Staphylococcus epidermidis*) has been chosen as the microorganism to test in the optimisation phase to determine the best configuration for the plasma system and assess its inactivation efficacy.

Given that in our previous study we had selected treatment times of 30 min, for this new investigation, we opted to conduct tests of 10 min, with the aim of minimising treatment time, from the perspective of process optimisation. The choice of treatment time also depends on the minimum logarithmic reduction of pathogen charge required by European standards. In fact, BS EN 13697:2015 + A1:2019 and BS EN 14885:2022 (BSI 2020, 2022) state that a satisfactory bacterial reduction should reach at least 4 logarithmic cycles for the traditional chemical disinfectants. Lacking a specific standard for innovative technologies, the authors choose to adopt the requirements for standard employed processes. The selected treatment time allowed the achievement of the target Log$R$.

As previously mentioned, three parameters have been separately and subsequently tested in order to optimise the operative conditions and the system configuration: treatment chamber volume (1), DC (2) and presence of mist inside the chamber (3). From the optimisation perspective, each parameter was tested, starting from the most efficient conditions displayed by the previous tests.

3.1.1. Effect of the treatment chamber volume. It was expected that the concentration of reactive species would increase as the volume decreases and that the inactivation efficacy would subsequently increase. Therefore, the first parameter assessed was the volume of the treatment chamber. Two volumes have been compared: 18.5 l (Wide) and 0.925 l (Narrow).

The fixed parameters set for these experiments were DC 10% and absence of mist (Dry).

With the aim of discussing the effect of the treatment chamber volume, tests similar to those previously published (Maccaferri *et al* 2023) using the Wide chamber were conducted. In this study, a Narrow treatment chamber was used, under identical operating conditions.

As expected, the OAS test results (figure 5(a)) displayed that the concentration of ozone (O_3) drastically increased, whereas the volume of the chamber decreased (Wide: 173.3 $\pm$ 18.64 ppm; Narrow: 2537.25 $\pm$ 67.3 ppm). No nitrogen dioxide (NO_2) was detected in this configuration since this plasma source does not produce detectable nitrogen species in DC 10%, as previously reported by (Maccaferri *et al* 2023).

Moreover, the microbial inactivation efficacy (figure 5(b)) is significantly higher in the smaller volume than in the wider one (Wide: Log$R$ 0.39 $\pm$ 0.10; Narrow: Log$R$ 1.16 $\pm$ 0.08), suggesting that there should be a dose-response effect related to the concentration of O_3, which is known to be an efficient antimicrobial agent (Rangel *et al* 2022).

3.1.2. Effect of DC. Once it was determined that a smaller volume of the treatment chamber increased the inactivation efficacy, the subsequent experiments were conducted with the narrow chamber.

To assess the effect of DC on RONS production and *S. epidermidis* inactivation, two DCs, DC 10% and DC 100%, have been compared. OAS results previously reported (Maccaferri *et al* 2023), show that in DC 10% O_3 was largely produced but no NO_x was produced, while NO_x was measured in higher concentrations than O_3 when working in DC 100%.

Similar to the wide chamber tests, for the narrow chamber, OAS results (figure 6(a)) displayed that increasing the DC leads to a decrease in O_3 net production and an increase in NO_2 production (DC 10%: 2537.25 $\pm$ 67.3 ppm O_3, 0 ppm NO_2; DC 100%: 258.17 $\pm$ 149.05 ppm O_3, 792.11 $\pm$ 72.65 ppm NO_2).

Antimicrobial efficacy tests in the narrow chamber (figure 6(b)) showed that the inactivation efficacy significantly increased when employing DC 100% rather than DC 10% (DC 10%: Log$R$ 1.16 $\pm$ 0.08; DC 100%: Log$R$ 2.78 $\pm$ 0.18),

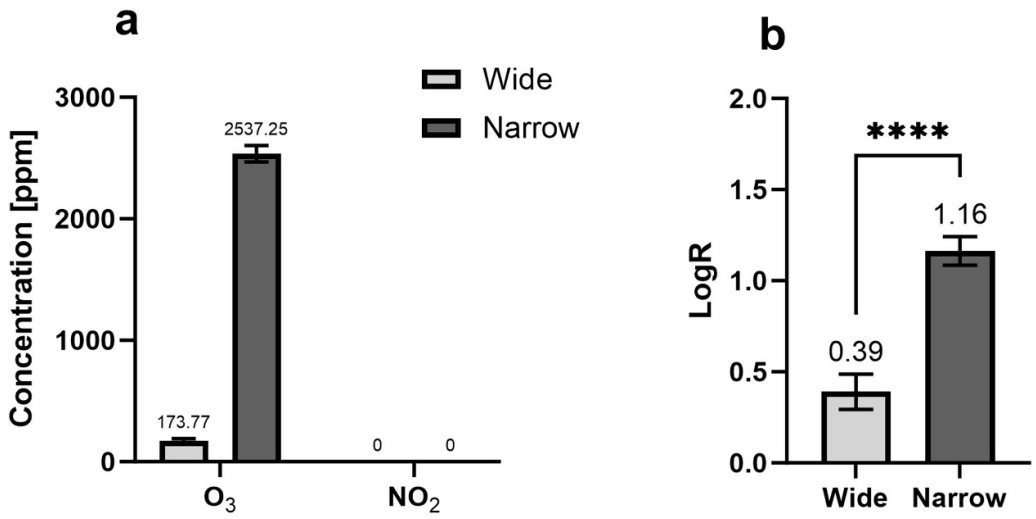

Figure 5. Comparison of reactive species concentration and microbial inactivation of *S. epidermidis* for different treatment chamber volumes (Wide: 18.5 l; Narrow: 0.925 l). Treatment conditions: DC 10%; Dry; $t = 10$ min. (a) Concentration of reactive species measured by OAS. (b) CFU Log reduction and SEM calculated from colony counts. $^{*} = P$-value < 0.05, $^{**} = P$-value < 0.001, $^{***} = P$-value < 0.0001, $^{****} = P$-value < 0.00001.

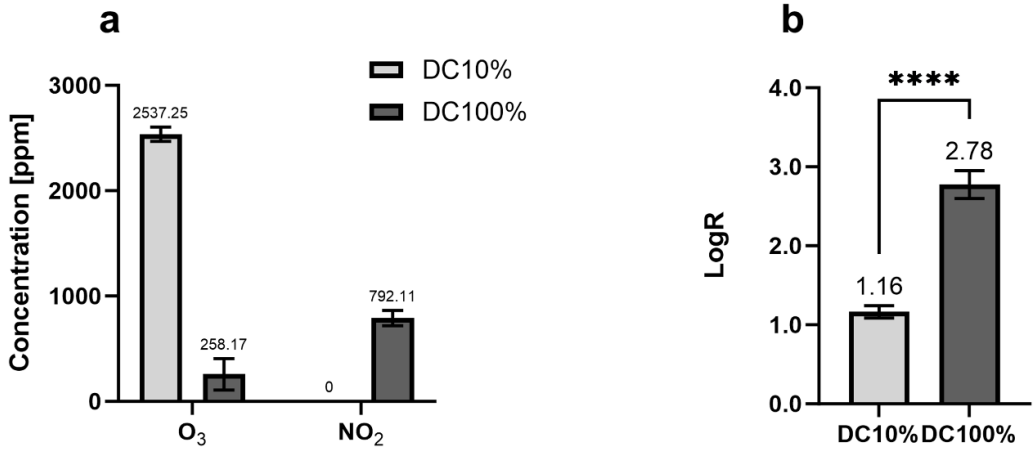

Figure 6. Comparison of reactive species concentration and inactivation of *S. epidermidis* for different duty cycles (DC 10%, DC 100%). Treatment conditions: Narrow chamber; Dry; t = 10 min. (a) Concentration of reactive species measured by OAS. (b) CFU Log reduction and SEM calculated from colony counts. * = P-value < 0.05, ** = P-value < 0.001, *** = P-value < 0.0001, **** = P-value < 0.00001.

leading to the belief that reactive nitrogen species are more effective than oxygen species.

These results suggest that O_3 is not the only agent implied in this source's inactivation effect. Moreover, it is known that gaseous NO_2 exposure has a strong bactericidal effect (Oh and Liu 2020), thus the bacterial load reduction in this regime could be influenced also by nitrogen reactive species production.

3.1.3. Effect of mist injection. Given the precedent results, the following experiments were conducted in a narrow chamber in DC 100% mode in order to optimise the antimicrobial efficacy.

It is known that in the presence of liquid water or humidity, plasma and gaseous species can react with H_2O molecules to generate different reactive species, among which some (e.g. hydrogen peroxide and peroxynitrite) have high antimicrobial activity (Stancampiano *et al* 2019). For this reason, it was chosen to compare *S. epidermidis* inactivation in treatments in ambient air (Dry) and in the presence of mist (Mist) by injecting aerosolised tap water in the chamber.

For technical matters, it is impossible to perform OAS experiments to determine the concentration of gaseous long-lived RONS. Up to the authors' knowledge, there have been no published studies regarding the feasibility of successfully employing OAS in the presence of aerosols, due to various obstacles, such as light beam diffusion and condensation (Nayak *et al* 2020).

The antimicrobial efficacy tests (figure 7) showed that the presence of mist significantly increased the inactivation effect (Dry: Log$R$ 2.78 $\pm$ 0.18; Mist: Log$R$ 3.50 $\pm$ 0.26), suggesting that gaseous species reacting with water molecules in aerosol droplets generate reactive species with high antimicrobial activity.

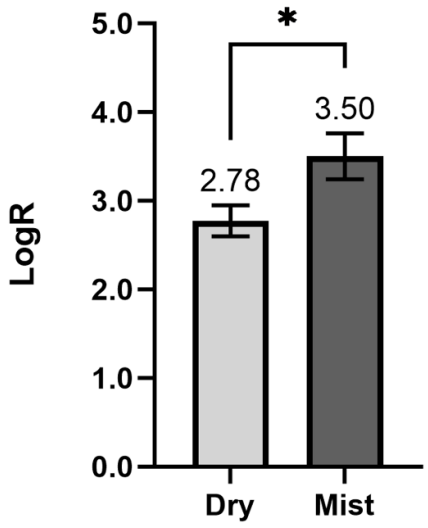

Figure 7. Microbial inactivation in the presence (Mist) or absence (Dry) of mist. Treatment conditions: narrow chamber; DC 100%; $t = 10$ min. CFU Log reduction and SEM were calculated from colony counts. * = P-value < 0.05, ** = P-value < 0.001, *** = P-value < 0.0001, **** = P-value < 0.00001.

3.2. Statistical analysis

On the basis of ANOVA, it was possible to observe that all the main factors significantly affected the response. Furthermore, when considering joint effects, only the combination of chamber size and DC yielded a significant impact. This finding, supported by a p-value analysis (table 2), is further illustrated in the factor effects plots presented in figure 8.

These plots offer valuable insights into both the individual and interactive effects of the examined factors. In accordance with the principles of Montgomery's 2^k factorial analysis, an absolute effect magnitude signifies a substantial influence on the process outcome. A positive effect sign denotes a positive correlation, indicating that transitioning from the low to high level of the factor results in an improved system response. Conversely, a negative effect sign suggests that optimising the response necessitates transitioning from the high to low level of the factor, adhering to the principles of factor optimisation within the factorial design framework.

Firstly, the negative effect (-1.68) observed for chamber volume (A) suggests that reducing the chamber size amplifies the biocidal action of the plasma system. This implies that a more confined space may intensify the concentration or distribution of reactive species, thus enhancing biocidal efficacy.

Conversely, the positive effects of mist (B) and DC (C), indicated by values of 0.52 and 0.87 respectively, signify improvements in response irrespective of other factors. The presence of mist likely facilitates the dispersion and interaction of reactive species with target contaminants, enhancing biocidal efficacy. Similarly, a higher DC, representing increased power input, correlates with enhanced plasma generation and subsequent biocidal activity.

Table 2. Effect values for main factorial effects (A, B, C) and their combinations.

Factorial effect	Effect	P- value
A	-1.68	2.72×10^{-10} *
B	0.52	6.14×10^{-04} *
AB	-0.23	0.082
C	0.87	2.36×10^{-06} *
AC	-0.71	2.54×10^{-05} *
BC	-0.05	0.665
ABC	-0.03	0.823

The asterisks indicate p-values less than 0.05, thus relative to significant effects.

Almost parallel segments in the factors effects plot, like in figure 8(c), represent a negligible interaction between the considered effects (C and B, i.e. DC and mist/dry condition), observable as well on the absolute value of effect BC, which is close to zero (-0.05), and on the p-value greater than 0.05 (0.665). Similarly, also the interaction AB between chamber volume and aerosol possible injection is negligible (effect -0.23, p-value 0.082, panel (a)) even though a slightly greater increase in effect value is displayed when injecting aerosol in the narrow chamber (A low), rather than in the wide chamber (A high).

Of particular interest is the interaction between chamber volume (A) and DC (C), which exhibits a significance comparable to that of the main factors since the effect appears to be of the same magnitude (-0.71, p-value 2.54×10^{-5}). This interaction suggests that the combined influence of chamber size and power input plays a critical role in determining biocidal efficacy. Notably while altering the DC with the wide chamber does not yield a significant difference, it confers considerable advantages with the narrow chamber. This implies that the impact of power input on biocidal action is more pronounced in a confined space, potentially due to increased residence time or enhanced plasma generation efficiency.

These findings underscore the intricate interplay between chamber size, mist presence, and DC in modulating the efficacy of the plasma system's biocidal action, highlighting the importance of considering multiple factors in optimising system performance.

3.3. Inactivation efficacy for Acinetobacter baumannii

After the optimisation phase, in which the best operative conditions and system configurations have been determined for *S. epidermidis* (a gram-positive bacterium), the optimised system has been tested to determine its efficacy in inactivating gram-negative bacteria both in Dry and Mist conditions. Particularly, *A. baumannii* has been chosen to perform the following experiments, and the results have been compared with those previously obtained with *S. epidermidis*.

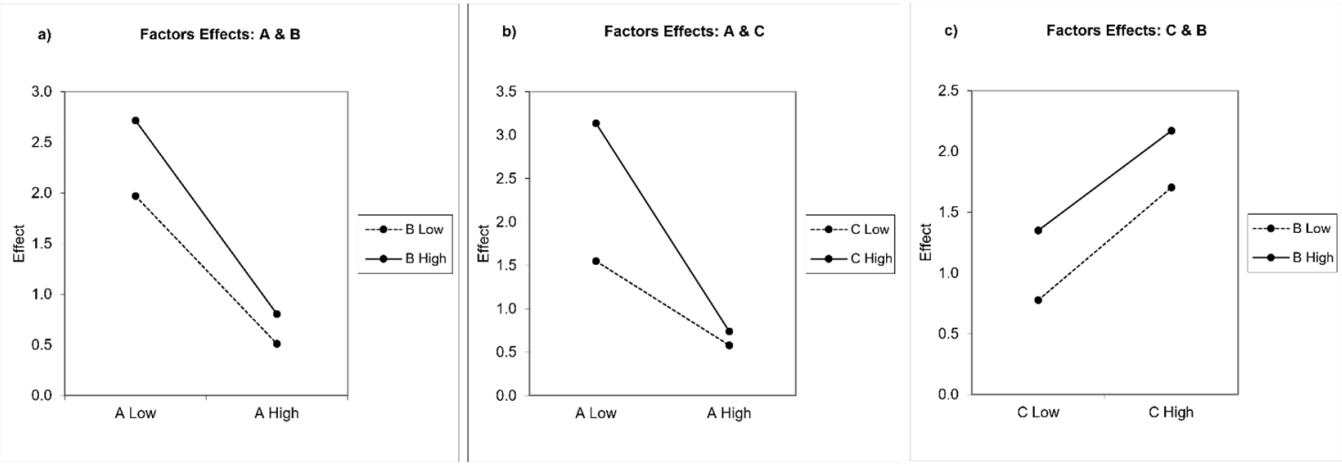

Figure 8. Evaluation of factors effects. (a) represents the correlation between chamber size and mist injection effects, (b) between chamber size and duty cycle effects, and (c) between duty cycle and mist injection effects.

For tests performed in the presence of mist, it was necessary to aerosolise DIW instead of tap water, since no colonies were grown from the recovery of *A. baumannii* control samples after tap water aerosolisation (results not shown).

Both 'Dry' and 'Mist' test results (figure 9) show that *A. baumannii* is more sensitive to the treatments than *S. epidermidis* (Dry: *S. epidermidis* Log*R* 2.78 ± 0.18; *A. baumannii* Log*R* 4.00 ± 0.08. Mist: *S. epidermidis* Log*R* 3.50 ± 0.26; *A. baumannii* Log*R* 4.73 ± 0.08.).

These results confirm that this plasma system and these configurations have good antimicrobial efficacy against gram-negative bacteria. Moreover, these results are coherent with other results, which show that gram-negative bacteria are commonly more susceptible to plasma treatments (Breijyeh *et al* 2023). Since the major difference between these two kinds of bacteria is the cell wall and plasma membrane configuration, it is expected that the effect of these treatments is related (at least partially) to the oxidative action of produced RONS on those cell components.

3.4. Effect of the reactive oxygen species (ROS)

Sodium thiosulphate ($Na_2S_2O_3$) is known to be an efficient ROS quencher thanks to its ability to react with O_3 (Yang *et al* 2020), thus it was decided to perform experiments aerosolising in the treatment chamber a water solution with a concentration of 5% w/v $Na_2S_2O_3$, in order to inhibit ROS biocidal effects and to better understand which reactive species are involved in the source microbial inactivation.

Firstly, the $Na_2S_2O_3$ effect for DC 10% (Ozone regime) for *S. epidermidis* was investigated to confirm that O_3 is the only antimicrobial factor in that regime. As expected, the inactivation effect is almost totally nullified (Mist: Log*R* 1.93 ± 0.64; Mist + $Na_2S_2O_3$: Log*R* 0.11 ± 0.06), remarking that in DC 10% the bacterial load reduction is entirely accomplished by O_3 (figure 10(a)).

Subsequently, we analysed how $Na_2S_2O_3$ affects microbial inactivation in DC 100% (NO_x regime) for both *S. epidermidis* and *A. baumannii*. Regarding *S. epidermidis*, the inactivation effect is partially inhibited by $Na_2S_2O_3$ ROS scavenging (Mist: Log*R* 3.50 ± 0.26; Mist + $Na_2S_2O_3$: Log*R* 1.43 ± 0.09) (figure 10(b)), showing that O_3 and its derived species are crucial to achieve the maximal effect, but that also NO_x and their derived species are importantly involved in the process. Regarding *A. baumannii*, $Na_2S_2O_3$ mist injection does not significantly affect the microbiocidal effect of the treatment (Mist: Log*R* 4.73 ± 0.08; Mist + $Na_2S_2O_3$: Log*R* 4.24 ± 0.08) (figure 10(c)), suggesting that NO_x and their derived species are sufficient to achieve a Log*R* higher than 4 (BSI (British Standards Institution) 2022, BSI (British Standards Institute) 2020).

Han *et al* reported that Gram-positive bacteria are mainly inactivated by damage to internal cell components, while Gram-negative bacteria are mainly inactivated by membrane damage and consequent cell leaking (2016), suggesting that *S. epidermidis* and *A. baumannii* should be inactivated by different mechanisms. Moreover, it is known that RNS has several targets on bacterial plasma membrane, whereas ROS mainly acts on intracellular targets (Fang 2004). All of these facts may explain the different inactivation efficiencies obtained by ROS scavenging during plasma treatments for *S. epidermidis* and *A. baumannii*.

3.5. Influence of temperature

The sample (and immediately surrounding air) temperatures were proven to show a maximum increase of about 5 °C with respect to the initial value (about 26 °C), when samples were exposed to a 10-min plasma treatment in the narrow chamber with DC 100% and Dry condition (figure 11).

The graphs show that in the narrow chamber the temperature is much more affected by the operating conditions than in the wide chamber. In fact, the samples are placed much

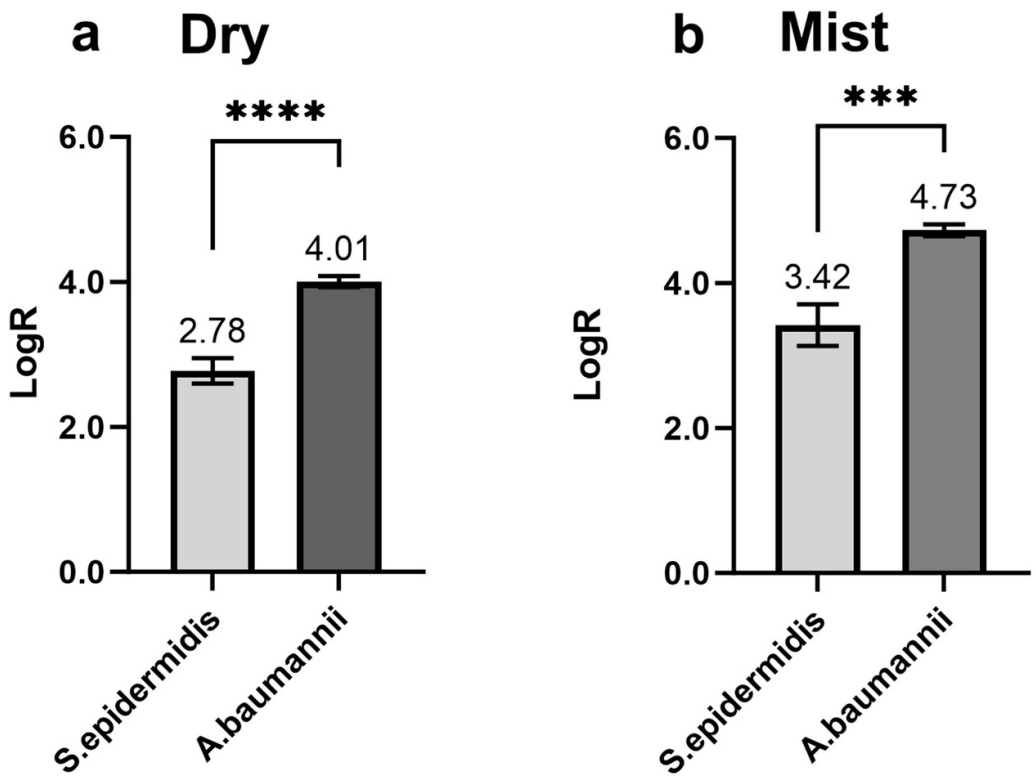

Figure 9. *A. baumannii* and *S. epidermidis* inactivation by the system operating in optimised conditions: Narrow chamber; DC 100%; $t = 10$ min. CFU log reduction and SEM were calculated from colony counts. (a) Dry air treatments. (b) Treatment in the presence of mist. $^{*} = P$-value < 0.05, $^{**} = P$-value < 0.001, $^{***} = P$-value < 0.0001, $^{****} = P$-value < 0.00001.

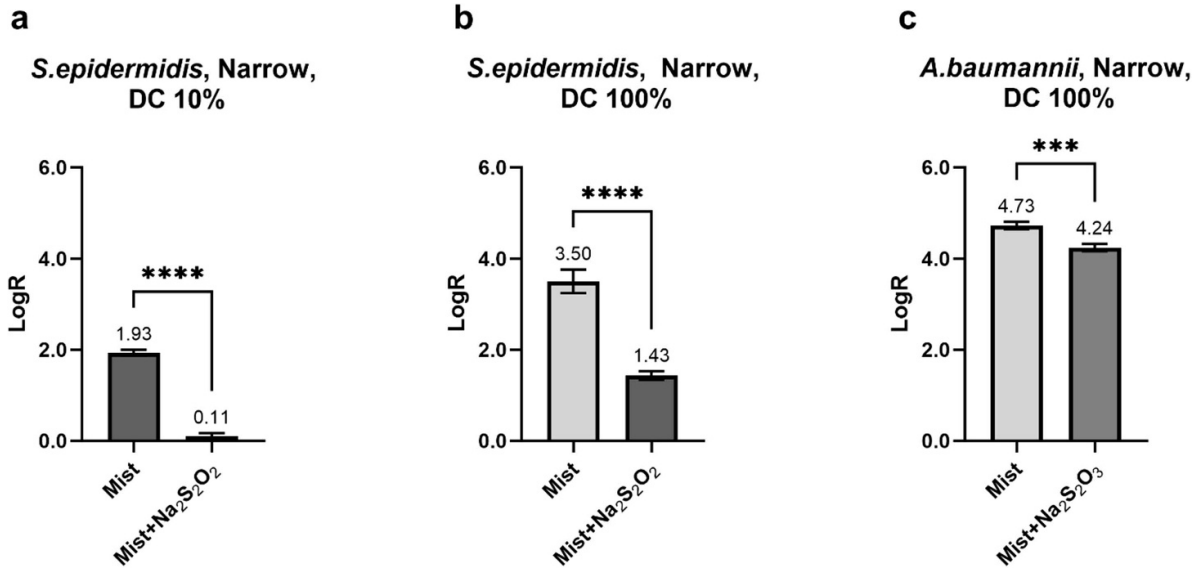

Figure 10. *S. epidermidis* and *A. baumannii* inactivation in the presence of mist and 5% w/v of $Na_2S_2O_3$ injected in the treatment chamber, for different duty cycles. Narrow chamber, $t = 10$ min. CFU log reduction and SEM were calculated from colony counts. (a) *S. epidermidis*, DC 10%. (b) *S. epidermidis*, DC 100%. (c) *A. baumannii*, DC 100%. $^{*} = P$-value < 0.05, $^{**} = P$-value < 0.001, $^{***} = P$-value < 0.0001, $^{****} = P$-value < 0.00001.

closer to the plasma generation surface, leading to a stronger and faster temperature increase, in particular with higher input power (DC 100%). A considerable decrease in temperature due to mist injection is observable during the very first minutes of treatment in the narrow chamber, both in DC 10% and DC 100%, while it is barely noticeable in the wide chamber. This is clearly explained by the difference in air volume, but also by the greater distance in the wide chamber between samples (and

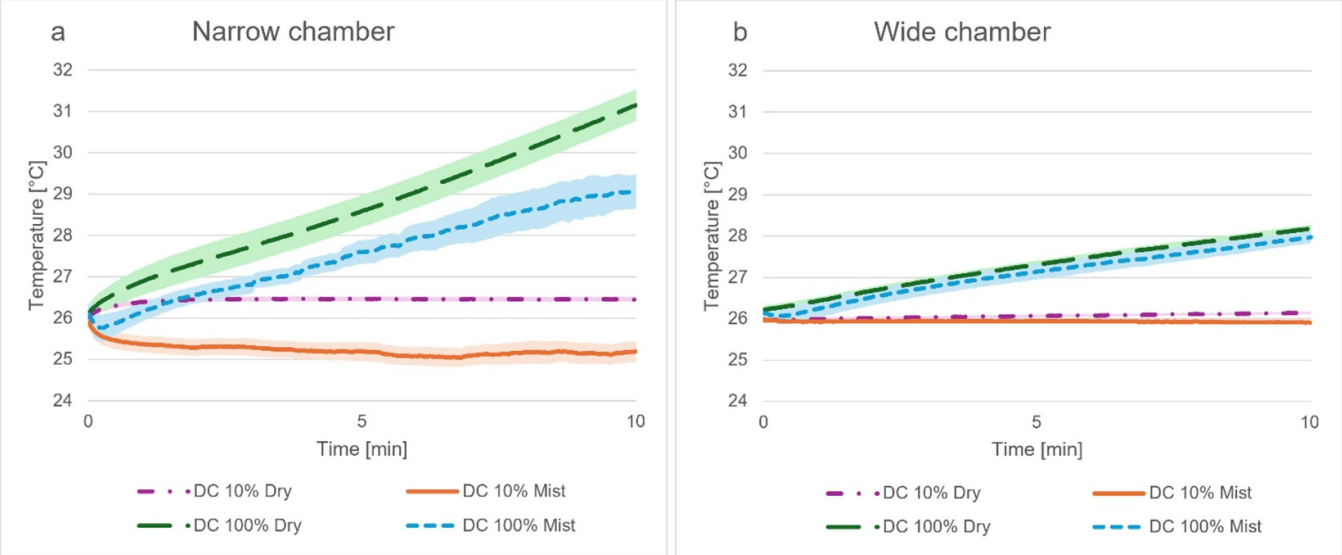

Figure 11. Average temperature of samples during 10-minute treatments in all the different operating conditions.

thus temperature probes) and the mist injector. After the first few minutes, high power settings (DC 100%) in both chambers display a continuous increase in temperature, induced by the Joule effect.

This result suggests that the temperature reached by the sample surfaces is kept sufficiently close to ambient conditions and it allows us to conclude that the viability of the microbial cells is not affected by the heat dissipated by the plasma discharge. This conclusion is made possible by comparing the growth range of the two bacterial strains to the measured temperature: *S. epidermidis* can grow until 46 °C (Willey *et al* 2008) and *A. baumannii* until 45 °C (Antunes *et al* 2011).

Furthermore, the temperature results confirm that the plasma-assisted sanitation process is suitable for heat-sensitive materials, among which polymeric films and containers constitute a large section of the food packaging industry.

4. Conclusions

This study presents the optimisation process of a plasma-assisted system for packaging decontamination. The described process led to a logarithmic inactivation rate of 3.5 in the case of gram-positive bacteria as contaminants and equal to 4.7 against gram-negative bacteria. The factors identified at each step that contributed to enhancing the biocidal action were the reduction of the treatment chamber volume, logically inducing higher concentrations of reactive species, and then setting a high DC in order to obtain higher powers and thus work in a nitrogen dioxide regime. This factor displays a volume-dependent behaviour, being particularly relevant in the narrow treatment chamber, while it is almost negligible in the wide one. Finally, the mist injection always resulted in being beneficial for the process, taking advantage of the presence of liquid-phase reactions and reactive species.

As expected, the system was proven effective against both gram-negative and gram-positive bacteria, pointing out that the bacteria included in the second category were found to be more sensitive to the treatments.

The optimisation path presented here is focused on industrialising an innovative process that is still relatively underexplored but exceedingly promising. The benefits of replacing traditional thermal or chemical methods for packaging decontamination with a plasma-assisted process have been outlined in the introduction, with economic advantages (utilisation costs being solely those of electrical energy) and sustainability implications (better environmental sustainability, requiring only electrical energy). However, despite the demonstrated efficacy as a proof of concept, very few studies have attempted to industrialise the process through scale-up and alignment with industrial requirements (Maccaferri *et al* 2024a). The plasma source used is one of the largest in the literature in terms of plasma generation surface and treatment chamber width, thus already geared towards scale-up. The statistical analysis presented, based on 2^k factorial analysis, is also crucial for identifying the minimum number of tests needed to gain a comprehensive understanding of the effect of different factors on the outcome of a process, as well as all combinations thereof. Ultimately, the approach taken in this investigation is innovative in its inclination towards industrial reality, which remains largely distant in this field of research. The next step will be the reactive species evaluation in liquid droplets (mist). The encouragement for the future is to increasingly gravitate towards industrial reality by developing and optimising the laboratory prototypes investigated so far, outlining specific development paths.

Data availability statement

All data that support the findings of this study are included within the article (and any supplementary files). All of these data are furthermore available in the following dataset created in order to comply with the provisions regarding FAIR data availability: https://doi.org/10.6092/unibo/amsacta/7938 (Maccaferri *et al* 2024b).

Acknowledgment

The PhD scholarship of the author Maccaferri, C was funded by IMA S.p.A. and by the European Union—NextGenerationEU through the Italian Ministry of University and Research under PNRR—Mission 4 Component 2, Investment 3.3 'Partnerships extended to universities, research centres, companies and funding of basic research projects' D M 352/2021—CUP J33C22001330009.

The PhD scholarship of Tomelleri, F is funded under the National Recovery and Resilience Plan (NRRP), Mission 4 Component 2 Investment 1.3- Call for tender No. 341 of 15 March 2022 of Italian Ministry of University and Research funded by the European Union—NextGenerationEU; Project code PE00000003, Concession Decree No. 1550 of 11 October 2022 adopted by the Italian Ministry of University and Research, Project title 'ON Foods—Research and innovation network on food and nutrition Sustainability, Safety and Security—Working ON Foods'.

Funding

The PhD scholarship of the author Maccaferri, C. is funded by IMA S.p.A. and by the European Union—NextGenerationEU through the Italian Ministry of University and Research under PNRR—Mission 4 Component 2, Investment 3.3 'Partnerships extended to universities, research centres, companies and funding of basic research projects' D.M. 352/2021—CUP J33C22001330009.

The PhD scholarship of Tomelleri, F. is funded under the National Recovery and Resilience Plan (NRRP), Mission 4 Component 2 Investment 1.3- Call for tender No. 341 of 15 March 2022 of Italian Ministry of University and Research funded by the European Union—NextGenerationEU; Project code PE00000003, Concession Decree No. 1550 of 11 October 2022 adopted by the Italian Ministry of University and Research, Project title 'ON Foods—Research and innovation network on food and nutrition Sustainability, Safety and Security—Working ON Foods'.

Statements and declarations

C M: Conceptualization, Methodology, Validation, Formal analysis, Investigation, Data curation, Writing—original draft preparation, Writing—review and editing, Visualization.

F T: Conceptualization, Methodology, Validation, Formal analysis, Investigation, Data curation, Writing—original draft preparation, Writing—review and editing, Visualization.

M G: Writing—review and editing, Supervision, Funding acquisition.

R L: Conceptualization, Methodology, Resources, Writing—review and editing, Supervision, Project administration, Funding acquisition.

ORCID iDs

Caterina Maccaferri https://orcid.org/0009-0004-7591-1367
Francesco Tomelleri https://orcid.org/0009-0006-7974-5364
Matteo Gherardi https://orcid.org/0000-0001-6995-6754
Romolo Laurita https://orcid.org/0000-0003-1744-3329

References

Antunes L C S, Imperi F, Carattoli A and Visca P 2011 Deciphering the multifactorial nature of acinetobacter baumannii pathogenicity *PLoS One* **6** e22674

Bauer A, Ni Y, Bauer S, Paulsen P, Modic M, Walsh J L and Smulders F J M 2017 The effects of atmospheric pressure cold plasma treatment on microbiological, physical-chemical and sensory characteristics of vacuum packaged beef loin *Meat. Sci.* **128** 77–87

Breijyeh Z, Jubeh B and Karaman R 2023 Resistance of gram-negative bacteria to current antibacterial agents and approaches to resolve it *Molecules* **28** 543

BSI (British Standards Institute) 2020 Chemical disinfectants and antiseptics—quantitative non-porous surface test for the evaluation of bactericidal and/or fungicidal activity of chemical disinfectants used in food, industrial, domestic and institutional areas—test method and requirements

BSI (British Standards Institution) 2022 Chemical disinfectants and antiseptics. application of european standards for chemical disinfectants and antiseptics p 76

Cadet J, Douki T and Ravanat J L 2011 Measurement of oxidatively generated base damage in cellular DNA *Mutat. Res.* **711** 3–12

Cadet J, Ravanat JL, TavernaPorro M, Menoni H and Angelov D 2012 Oxidatively generated complex DNA damage: tandem and clustered lesions *Cancer Lett.* **327** 5–15

Cahill O J, Claro T, O'Connor N, Cafolla A A, Stevens N T, Daniels S and Humphreys H 2014 Cold air plasma to decontaminate inanimate surfaces of the hospital environment *Appl. Environ. Microbiol.* **80** 2004–10

Deng S, Cheng C, Ni G, Meng Y and Chen H 2010 Bacillus subtilis devitalization mechanism of atmosphere pressure plasma jet *Curr. Appl. Phys.* **10** 1164–8

Edelblute C M, Malik M A and Heller L C 2016 Antibacterial efficacy of a novel plasma reactor without an applied gas flow against methicillin resistant Staphylococcus aureus on diverse surfaces *Bioelectrochemistry* **112** 106–11

European Food Safety Authority 2023 The european union one health 2022 zoonoses report *EFSA J.* **21** e8442

Fang F C 2004 Antimicrobial reactive oxygen and nitrogen species: concepts and controversies *Nat. Rev. Microbiol.* **2** 820–32

Feizollahi E, Misra N N and Roopesh M S 2021 Factors influencing the antimicrobial efficacy of dielectric barrier discharge (DBD) atmospheric cold plasma (ACP) in food processing applications *Crit. Rev. Food Sci. Nutr.* **61** 666–89

Govaert M *et al* 2018 Resistance of L. monocytogenes and S. Typhimurium towards cold atmospheric plasma as function of biofilm age *Appl. Sci.* **8** 2702

Hähnel M, Von Woedtke T and Weltmann K D 2010 Influence of the air humidity on the reduction of Bacillus spores in a defined environment at atmospheric pressure using a dielectric barrier surface discharge *Plasma Process. Polym.* **7** 244–9
Han L, Patil S, Boehm D, Milosavljević V, Cullen P J and Bourke P 2016 Mechanisms of inactivation by high-voltage atmospheric cold plasma differ for Escherichia coli and Staphylococcus aureus *Appl. Environ. Microbiol.* **82** 450–8
Hoover L 2001 *Food Packaging* (Flexo) pp 26–31
Hu M and Guo Y 2012 The effect of air plasma on sterilization of escherichia coli in dielectric barrier discharge *Plasma Sci. Technol.* **14** 735–40
İbiş F, Oflaz H and Ercan U K 2016 Biofilm inactivation and prevention on common implant material surfaces by nonthermal DBD plasma treatment *Plasma Med.* **6** 33–45
Kim J S, Lee EJ, Choi E H and Kim YJ 2014 Inactivation of Staphylococcus aureus on the beef jerky by radio-frequency atmospheric pressure plasma discharge treatment *Innovative Food Sci. Emerg. Technol.* **22** 124–30
Kleinschmidt S, Huygens F, Faoagali J, Rathnayake I U and Hafner L M 2015 Staphylococcus epidermidis as a cause of bacteremia *Future Microbiol.* **10** 1859–79
Kordová T, Scholtz V, Khun J, Soušková H, Hozák P and Čeřovský M 2018 Inactivation of microbial food contamination of plastic cups using nonthermal plasma and hydrogen peroxide *J. Food Qual.* **2018** 1–7
Kovalová Z *et al* 2013 Decontamination of Streptococci biofilms and Bacillus cereus spores on plastic surfaces with DC and pulsed corona discharges *EPJ Appl. Phys.* **61** 2024
Kramer B, Hasse D, Guist S, Schmitt-John T and Muranyi P 2020 Inactivation of bacterial endospores on surfaces by plasma processed air *J. Appl. Microbiol.* **128** 920–33
Kramer B, Warschat D and Muranyi P 2022 Disinfection of an ambulance using a compact atmospheric plasma device *J. Appl. Microbiol.* **133** 696–706
Kramer B, Wunderlich J and Muranyi P 2016 Impact of pulsed light on cellular activity of Salmonella enterica *J. Appl. Microbiol.* **121** 988–97
Leduc M, Guay D, Leask R L and Coulombe S 2009 Cell permeabilization using a non-thermal plasma *New J. Phys.* **11** 115021
Lee HB *et al* 2011 비열 플라즈마 처리를 이용한 polystyrene, 소시지 케이싱, 그리고 훈제연어에서의 식중독균 저해 Inhibition of Foodborne Pathogens on Polystyrene, Sausage Casings, and Smoked Salmon Using Nonthermal Plasma Treatments *J. Food Sci. Technol.* **43** 513–7
Maccaferri C, Gherardi M and Laurita R 2024a Evaluating atmospheric pressure cold plasma decontamination techniques for packaging materials : a systematic review and meta-analysis *Front. Phys.* **12** 1399720
Maccaferri C, Sainz-García A, Capelli F, Gherardi M, Alba-Elías F and Laurita R 2023 Evaluation of the antimicrobial efficacy of a large-area surface dielectric barrier discharge on food contact surfaces *Plasma Chem. Plasma Process.* **43** 1773–90
Maccaferri C, Tomelleri F, Gherardi M and Laurita R 2024b Data related to the optimisation of plasma process for decontamination of bacterial contaminants on polymeric food packaging materials (University of Bologna)
Mandal R, Singh A and Pratap Singh A 2018 Recent developments in cold plasma decontamination technology in the food industry *Trends Food Sci. Technol.* **80** 93–103
Moiseev T, Misra N N, Patil S, Cullen P J, Bourke P, Keener K M and Mosnier J P 2014 Post-discharge gas composition of a large-gap DBD in humid air by UV-Vis absorption spectroscopy *Plasma Sources Sci. Technol.* **23** 065033
Montgomery D C 2013 Response surface methods and designs *Design and Analysis of Experiments* (Wiley) ch 11
Muranyi P, Wunderlich J and Langowski H C 2010 Modification of bacterial structures by a low-temperature gas plasma and influence on packaging material *J. Appl. Microbiol.* **109** 1875–85
Nayak G, Andrews A J, Marabella I, Aboubakr H A, Goyal S M, Olson B A, Torremorell M and Bruggeman P J 2020 Rapid inactivation of airborne porcine reproductive and respiratory syndrome virus using an atmospheric pressure air plasma *Plasma Process. Polym.* **17** 1–15
Noriega E, Shama G, Laca A, Díaz M and Kong M G 2011 Cold atmospheric gas plasma disinfection of chicken meat and chicken skin contaminated with Listeria innocua *Food Microbiol.* **28** 1293–300
Oh S and Liu Y B 2020 Effectiveness of nitrogen dioxide fumigation for microbial control on stored almonds *J. Food Prot.* **83** 599–604
Piergiovanni L and Limbo S 2017 *Tecnologie di packaging per la qualità degli alimenti, Tecnologie di packaging per la qualità degli alimenti* (Springer) (https://doi.org/10.1007/978-88-470-1457-2)
Rangel K *et al* 2022 Detrimental effect of ozone on pathogenic bacteria *Microorganisms* **10** 1–17
Salgado B A B, Fabbri S, Dickenson A, Hasan M I and Walsh J L 2021 Surface barrier discharges for Escherichia coli biofilm inactivation: modes of action and the importance of UV radiation *PLoS One* **16** 1–19
Simoncelli E, Schulpen J, Barletta F, Laurita R, Colombo V, Nikiforov A and Gherardi M 2019 'UV-VIS optical spectroscopy investigation on the kinetics of long-lived RONS produced by a surface DBD plasma source *Plasma Sources Sci. Technol.* **28** 095015.1–095015.13
Sipoldova Z Š and MacHala Z 2011 Biodecontamination of plastic and dental surfaces with atmospheric pressure air DC discharges *IEEE Trans. Plasma Sci.* **39** 2970–1
Stancampiano A *et al* 2019 Plasma and aerosols: challenges, opportunities and perspectives *Appl. Sci.* **9** 3861
Szili E J *et al* 2017 The assessment of cold atmospheric plasma treatment of DNA in synthetic models of tissue fluid, tissue and cells *J. Phys. D: Appl. Phys.* **50** 274001
Takai E, Kitamura T, Kuwabara J, Ikawa S, Yoshizawa S, Shiraki K, Kawasaki H, Arakawa R and Kitano K 2014 Chemical modification of amino acids by atmospheric-pressure cold plasma in aqueous solution *J. Phys. D: Appl. Phys.* **47** 285403
Tučeková Z K *et al* 2021 Multi-hollow surface dielectric barrier discharge for bacterial biofilm decontamination *Molecules* **26** 910
Tučeková Z, Koval'ová Z, Zahoranová A, Machala Z and Černák M 2016 Inactivation of Escherichia coli on PTFE surfaces by diffuse coplanar surface barrier discharge *EPJ Appl. Phys.* **75** 2024
WHO 2014 Foodborne diseases (available at: www.who.int/foodsafety/areas_work/foodborne-diseases/en/)
Willey J M, Sherwood L M and Woolverton C J 2008 *Prescott, Harley and Klein's Microbiology 7th* edn
Yang J, Luo C, Li T, Cao J, Dong W, Li J and Ma J 2020 Superfast degradation of refractory organic contaminants by ozone activated with thiosulfate: efficiency and mechanisms *Water Res.* **176** 115751
Yun H, Kim B, Jung S, Kruk Z A, Kim D B, Choe W and Jo C 2010 Inactivation of Listeria monocytogenes inoculated on disposable plastic tray, aluminum foil, and paper cup by atmospheric pressure plasma *Food Control.* **21** 1182–6
Yusupov M, Van der Paal J, Neyts E C and Bogaerts A 2017 Synergistic effect of electric field and lipid oxidation on the permeability of cell membranes *Biochim. Biophys. Acta* **1861** 839–47
Zimmerman M, Peterson N A and Zimmerman M A 2016 Beyond the individual : toward a nomological network of organizational empowerment beyond the individual : toward a nomological network of organizational empowerment 34 p 2024